Optics & Laser Technology 139 (2021) 106900

Contents lists available at ScienceDirect

Optics and Laser Technology

journal homepage: www.elsevier.com/locate/optlastec

Full length article

Smart-phone phase contrast microscope with a singlet lens and deep learning

Yinxu Bian [a], Yannan Jiang [b], Yuran Huang [c,d], Xiaofei Yang [e], Weijie Deng [f,g], Hua Shen [a,h], Renbing Shen [b,*], Cuifang Kuang [c,d,*]

[a] School of Electronic and Optical Engineering, Nanjing University of Science and Technology, Nanjing 210094, China
[b] Department of General Surgery, The Affiliated Suzhou Hospital of Nanjing Medical University, Suzhou Municipal Hospital, Suzhou 215002, China
[c] State Key Laboratory of Modern Optical Instrumentation, Zhejiang University, Hangzhou 310027, China
[d] College of Optical Science and Engineering, Zhejiang University, Hangzhou 310027, China
[e] School of Optoelectronic Science and Engineering & Collaborative Innovation Center of Suzhou Nano Science and Technology, Soochow University, Suzhou 215006, China
[f] Changchun Institute of Optics, Fine Mechanics and Physics, Chinese Academy of Sciences, Changchun 130033, China
[g] Key Laboratory of Optical System Advanced Manufacturing Technology, Chinese Academy of Sciences, Changchun 130033, China
[h] Department of Material Science and Engineering, University of California Los Angeles, Los Angeles, CA 90095, USA

ARTICLE INFO

Keywords:
Computation imaging
Microscopy
Aspheric lens design
Deep learning

ABSTRACT

Amounts of cost-effective biological observing and detecting instruments are needed in biology and medical applications. In these demands, a low-cost, portable microscope with light-weight and tele-communication, is very attractive in the resource-limit area. In this manuscript, a portable singlet phase contrast microscope based on smart-phones are proposed. In the optics hardware, an external singlet lens is designed and closely attached before the rear cameras of a smart-phone, which constructs the imaging part of a simplified microscope. And a circular oblique illumination is adopted. In the computational imaging part, the in-focus images recorded by the smart-phone are virtually enhanced and style-transferred to phase contrast images by deep learning methods. Through pairs of experimental image data, we train the deep learning network and demonstrate the effectiveness of this virtual phase contrast imaging approach using multiple samples, e.g., unstained/transparent tumor tissue pathological slide, and H&E (Hematoxylin and Eosin) stained tumor tissue pathological slide. Our results provide a powerful example of low-cost portable phase contrast microscope with high-speed tele-communication abilities in the 5G + mobile internet era.

1. Introduction

Commercial microscopes are widely used for diagnosis in biological and medical applications. These microscopes are expensive and bulky with precise optics configurations and must be fixed in a research-level environment, which is difficultly acquired in resource-limited areas. Thus, in recent years, low-cost portable microscopes based on smart-phone, attract researchers and engineers' focus. These low-cost portable microscopes make full use of the consumer electronic product's advantages, including the cameras, the tele-communication ability, the software applications (APPs) eco-system, the low price and so-on [1–6]. Thanks to former efforts, smart-phone microscopes have demonstrated its promise as a powerful micro-level imaging tool for bio-sample, e.g., medical pathologic slides. As the attractive advantages of free-from-assembling and light-weight-package, singlets imaging/microscopy is also a hot optical topic [7–11]. In contrast to multiple-piece lens, many industrial procedures about assembling and measurements are exempt in a singlet lens. Freeform-surface lens, diffractive-surface lens, meta-material lens and meta-surface lens have been developed to achieve singlet imaging [10,11]. In reported portable smart-phone microscopes, reversed cell-phone lens, commercial microscope objectives and reversed short-focal-length monitoring lens are used in smart-phone microscopes, which all functions as the objective lens [5,12–15]. These 'objective lens' are still different kinds of multiple-piece lens, which cannot essentially reduce industrial costs and procedures about assembling and measurements. Besides, these 'objective lens' are not initially designed for smart-phone microscope, where the field of view (FOV) is limited and vignetting exists as the field and aperture mismatch. In this

* Corresponding authors at: State Key Laboratory of Modern Optical Instrumentation, Zhejiang University, Hangzhou 310027, China (C. Kuang).
E-mail addresses: 13862031461@qq.com (R. Shen), cfkuang@zju.edu.cn (C. Kuang).

https://doi.org/10.1016/j.optlastec.2020.106900
Received 24 October 2020; Received in revised form 16 December 2020; Accepted 30 December 2020
Available online 6 February 2021

manuscript, we propose an aspheric singlet lens as the extensible lens attached before the rear camera lens of the smart-phone.

In the resource-limited area, chemical dyeing is another difficult work, which costs time, well-trained labor and chemical reagent/instruments. After chemical dyeing, the tissue/cell would be observed easily and colorfully under a basic brightfield microscope. It is very popular and attractive for microscopic analysis by bio/medical experts. Besides, chemical dyeing would kill the cells, which cannot observe biological and medical specimens in vitro. Free from chemical dyeing, phase contrast microscopy (PCM) is invented for transparent and weakly scattering sample [16–25]. PCM provides phase information about the refractive index distribution of transparent specimens. The best advantage of PCM is that it does not require any chemical dyeing or fluorescent labelling. Although it seems to provide a microscopy technology to observe specimens without labelling and staining, microscopes relating with PCM are with complex optical configurations and computing time cost. Zernike phase contrast (ZPC) microscopes need an inset circular Zernike phase plate at the Fourier spectrum of the microscope objective lens [16]. Differential interference contrast (DIC) microscopes [17] need a fine assembled birefringent crystal, e.g., Wollaston prism. And other quantitative phase imaging (QPI) microscopes could get the quantitative phase of the sample, which mainly include the interference holography and computational QPI methods. The interference holography QPI technologies are based on two-path interferometer configurations, which are very complex and sensitive to the environment noise. In contrast, the computational QPI technologies [18–25] are cost-effective, such as transport-of-intensity equation (TIE), G-S phase retrieval iterations and Fourier ptychographic microscopy (FPM) and deep learning methods. Among them, deep learning methods show the potential to reduce the computing time much. In this manuscript, we propose an image-style-transfer deep learning method to get virtual phase contrast images for our smart-phone microscope.

There are two highlights, covering the optics hardware and the computational imaging method, are introduced in this manuscript. In optics hardware, a designed singlet aspheric lens is attached before the rear cameras of the smart-phone, which works as the function of a microscope objective lens. Our designed aspheric singlet lens keeps the same modulation transfer function (MTF) curves across all FOVs, which is very important in signal processing methods. Different from the brightfield microscopy and above mentioned computationally modulating illuminations, the quasi-monochromatic circular oblique light is adopted. After recording by the smart-phone camera, the picture data are transmitted to the computer by the 5G/WIFI telecommunication. In the computational imaging part, the picture is virtually enhanced to a phase contrast image by the image-style-transfer deep learning method, without any inset Zernike phase plate.

In the following contents, firstly, we introduce the principle and guidelines to achieve our smart-phone phase contrast microscope. Secondly, the singlet aspheric lens, functioning as the objective lens, is designed and analyzed. Thirdly, a generative adversarial network (GAN) based deep learning method is stated. Fourthly, we demonstrate the effectiveness of this virtual phase contrast imaging approach using multiple samples, e.g., unstained/transparent tumor tissue pathological slide, and H&E (Hematoxylin and Eosin) stained tumor tissue pathological slide. In final, some limits, assumptions and explanations are discussed.

2. Theory and method

2.1. Zernike phase contrast

Presented in Fig. 1 is a cut-away diagram of a phase contrast microscope [16]. Partially coherent illumination produced by a light source, e.g., LED and halogen lamp, is directed through a collector lens and focused on a specialized annulus. The annulus is at the front focal plane of the substage condenser. After passing through the annulus and the substage condenser, the light wavefront is modulated by the specimen. The wavefront is diffracted and retarded in phase by structures and phase gradients of the specimen. However, when the specimen is transparent, most of the energy is still undeviated background light. The modulated information light and the background light are both collected by the microscope objective lens. But they are segregated at the rear focal plane by a phase plate at the Fourier spectrum plane. Finally, a phase contrast image is observed in the CMOS image sensor.

2.2. Virtual phase contrast microscopy

In contrast to Fig. 1, we propose a cost-effective virtual phase contrast microscopy, whose hardware and working flow are illustrated in Fig. 2. As shown in Fig. 2 (a), the illumination part is almost same with that in Fig. 1. The illumination is a blue LED. However, a designed aspheric singlet lens is as the microscope objective lens, which is closely put before the rear camera of a smart-phone. The rear camera equals to the combination of the tube lens and the CMOS image sensor (in Fig. 1). The working flow is shown in Fig. 2 (b). The working flow are typed as ‘training flow’, which is expressed as the black arrow and ‘practical working flow’, which is expressed as the blue arrow. In the training flow, firstly, a set of images, i.e. I_0, are recorded by our smart-phone microscope. Secondly, I_0 are formatted into grey images, and are enhanced as I_1 by the deep learning deconvolution reported in Ref [26]. Another image set of the same bio-sample, i.e. I'_1, are recorded by a research-level Zernike phase contrast microscope, whose principle is same with that in Fig. 1. Thirdly, I_1 and I'_1 are digitally resolution-scaled and registered. Fourthly, the style-transfer DNN kernel is iteratively trained, where I_1 is the ‘input data’ and I'_1 is the ‘real data’. The style-transfer DNN training details would be explained in Section 2.4. After the

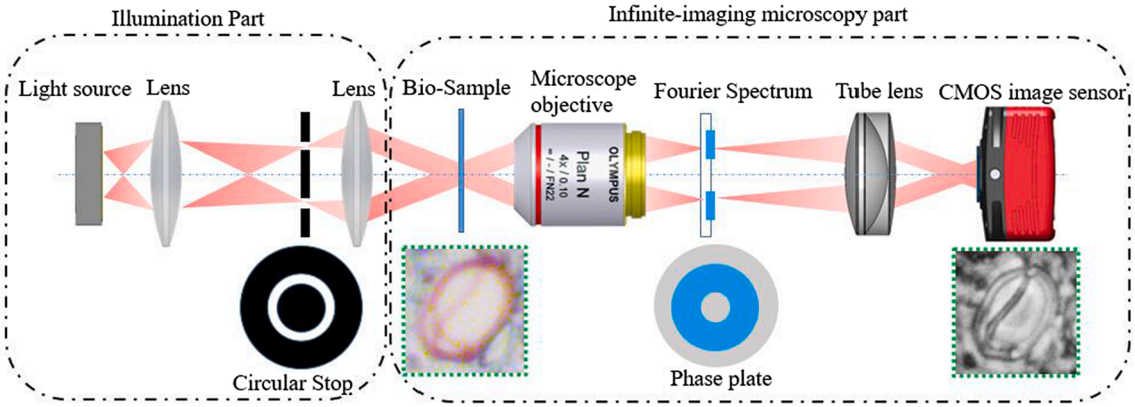

Fig. 1. Schematic of traditional Zernike phase contrast microscopy.

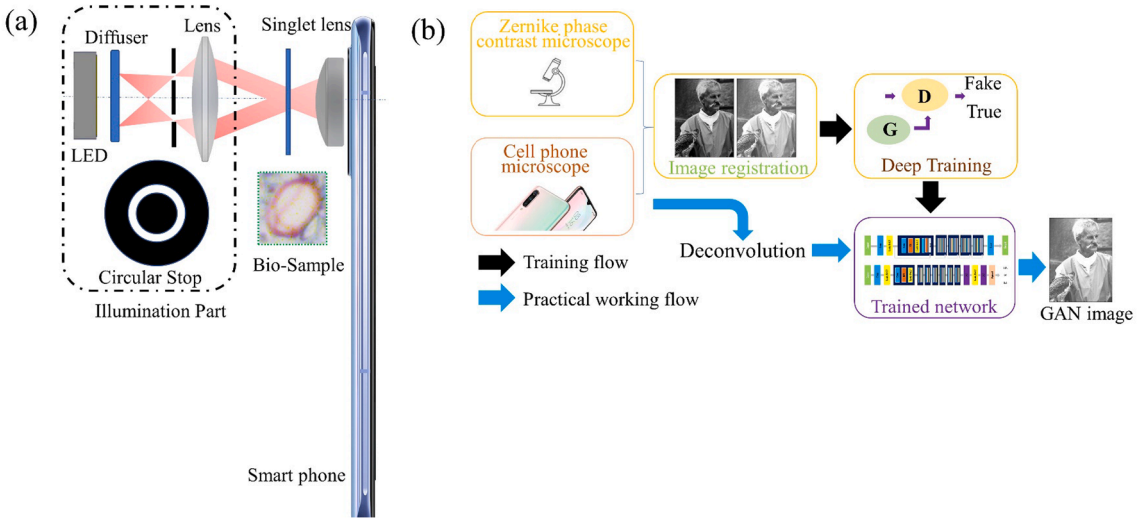

Fig. 2. Virtual phase contrast microscopy based on a smart-phone and an aspheric singlet objective lens. (a) Schematic of the setup. (b) Working flowchart based on deep learning style-transfer method.

style-transfer DNN kernel is got, it would be used in the 'practical working flow', which is shown as the blue arrow in Fig. 2 (b). By the style-transfer deep convolution, we would achieve the high-contrast virtual phase contrast imaging of the transparent bio-samples.

2.3. Singlet aspheric lens

Effects of the optical imaging system aberrations can be described as the Normalized Modulation Transfer Function (NMTF), which can quantify the signal transferring performance exactly. A singlet lens cannot eliminate aberrations across a large FOV. A low NMTF value means a low contrast, but the spatial frequency still could pass the lens. The spatial frequency is usually limited by the cut-off spatial frequency. And a linear signal imaging system helps computational imaging methods. Thus, we design a singlet lens for our smart-phone phase contrast microscope, whose characteristics should be: (1) a linear signal imaging system; (2) the cut-off frequency should be close to the diffraction-limited cut-off frequency. As shown in Fig. 3(a), we design

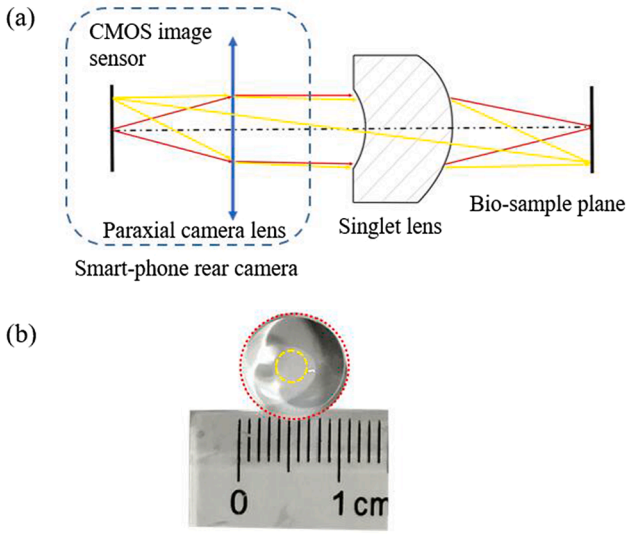

Fig. 3. Aspheric singlet lens. (a) Optical design schematic. (b) Photograph: the effective aspheric area is in the yellow circle, and the circular area between the yellow circle and the red circle is the mechanical supporting part. It is made of E48R.

the aspheric singlet lens in a reversed optical path. The CMOS image sensor is viewed as the object plane. The complex rear camera of the smart-phone is effectively simplified as a paraxial ideal lens, as its aberrations are balanced. The design targets are: the effective focal length is $f = 10$ mm, NA $= 0.1$ and the FOV is ± 2.5 mm. After the 'initial-build' and 'iterative optimization' steps [26], we designed the singlet lens successfully, which is expressed as Eq. (1) and shown in Fig. 3.

$$Z = \frac{cr^2}{1+\sqrt{1-(1+k)c^2r^2}} + \alpha_1 r^2 + \alpha_2 r^4 + \alpha_3 r^6 + \alpha_4 r^8 + \alpha_5 r^{10} \quad (1)$$

where c is the curvature ($1/R$), k is the aspheric coefficient, and α is high order terms coefficients. The photograph of the singlet lens is Fig. 3(b), the effective aspheric area is in the yellow circle, where the maximum aperture is 3 mm. And the circular area between the yellow circle and the red circle is the mechanical supporting part, where the diameter of the red circle is 10 mm. And the manufacture details are shown in Fig. 4. The singlet lens material is E48R, which is provided by ZEON Corp, JAPAN. The RMS surface error of both surfaces should be less than $\lambda/3$ ($\lambda = 632$ nm). Both their centration should be less than 1 arcmin. Their surface qualities should be better than 60–30 scratch-dig. And the surface roughness (RMS Rq) should be less than 5 nm. The effective aperture of the first surface is 2 mm, and that of the second surface is 3 mm. And the center thickness is 2.02 mm.

Fig. 5(a) is about the NMTF curves of our designed lens. The NMTF curves at all FOVs (0–2.5 mm) are consistent. Although the NMTF curves are all lower than the diffraction limit NMTF curve, the singlet lens keeps the linear signal imaging properties, which is helpful for the deep learning deconvolution and deep learning style-transfer methods. In contrast, shown in Fig. 5(b), the designed aspheric singlet lens, which is constructed by optimizing the spot radius values of all FOVs, has a degrading NMTF with the FOV increasing. This means it is difficult to get a linear signal imaging system by the traditional aspheric singlet lens designing method, i.e., optimizing the spot radius values.

2.4. GAN deep learning image-style-transfer

Deep learning style-transfer methods has been used to transfer the style of a reference style photo onto another input picture [27–39], which have been applied into biomedical images [27–36], virtual color stain [37–38] and so on. In our method, we also design a DNN network to transfer the images recorded by the smart-phone to the phase contrast style. The DNN network cannot produce new textures, structures and information, but could improve the contrast of original recorded images.

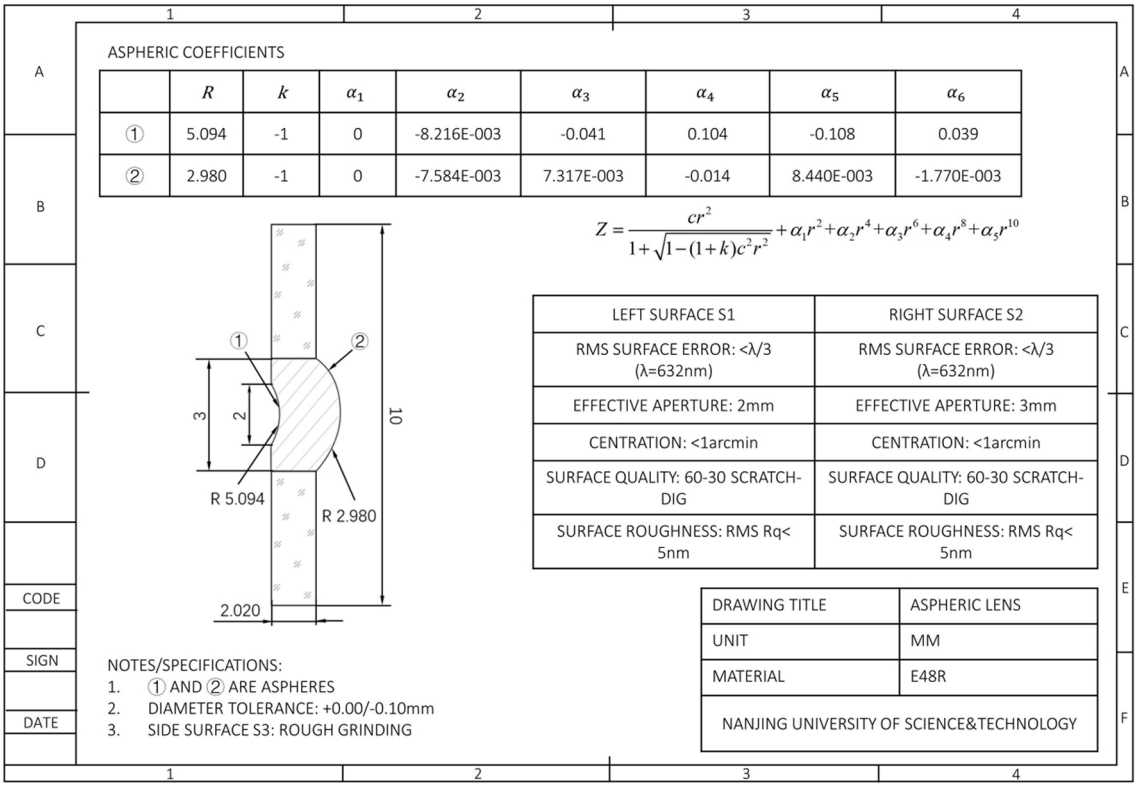

Fig. 4. Engineering draw of our designed aspheric singlet lens with manufacturing details.

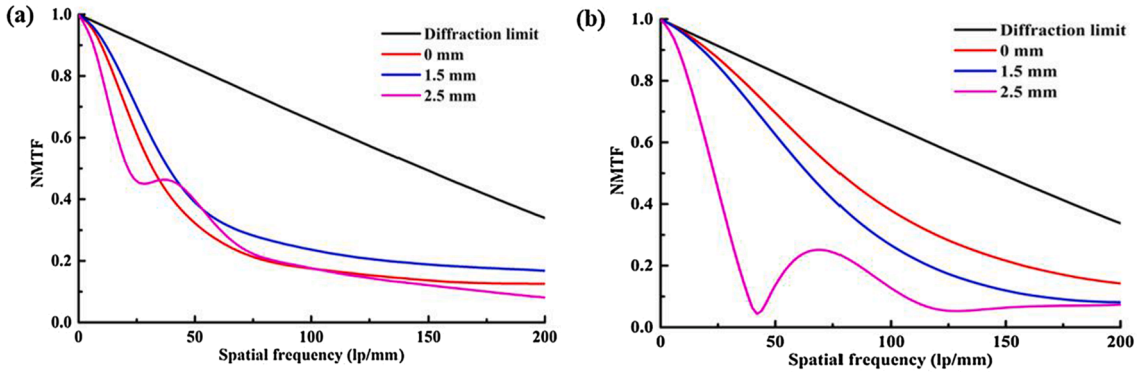

Fig. 5. NMTF comparison of our aspheric singlet lens and a conventional even aspheric lens. (a) NMTF of our aspheric singlet lens. (b) NMTF of a conventional even aspheric lens, which is construct by optimizing the spot radius values of all FOVs.

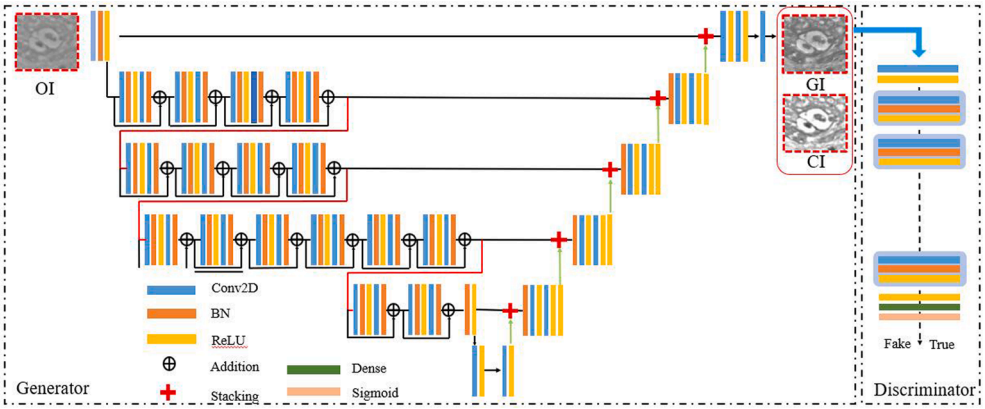

Fig. 6. A U-net GAN network to achieve deep learning image-style-transfer.

Our idea is inspired by the exiting image-style-transfer deep learning methods and their DNN networks [28–39]. To prevent painting-like distortions, wiggly edges, wavy textures, and make full use of the original image features, we use the U-net network structure with residual learning and skip connections, which is shown in Fig. 6. Following the digital registration and deep learning deconvolution, the image pairs are partitioned to overlapping patches of 256 × 256 pixels. And 2048 pairs data are for training, and 100 pairs data are for testing. Then they are input to a GAN model for deep training. The GAN consists of a generator network (GN) and a discriminator network (DN), which are both deep convolution networks and contest with each other in the form of a dynamic zero-sum game. The DN consists of a Conv2D layer, 7 Dense blocks, a ReLU layers, a Dense layer and a Sigmoid layer. And the DN output is a BOOL value (fake or true). The DN's loss function is given by:

$$l_{DN} = D(G(I_{GI}))^2 + (1 - D(I_{CI}))^2, \quad (2)$$

where D(.) is the DN convolution operating and G(.) is the GN convolution operating. In Fig. 6 and Eq. (2), the I_{GI} is the output data of the GN; the I_{OI} is the input data of the GN, which is the deconvoluted smartphone microscope data; and I_{CI} is "ground truth" of the DN, which is the Zernike phase contrast microscopy images. In the dynamic zero-sum contesting game, GN tries to output/generate images as same statistical features as I_{CI}. In contrast, DN tries to distinguish the GN output image and the 'ground truth'. For the GN, we adapted the U-net architecture, which consists of a down-sampling path, skip stackings and an up-sampling path. In the down-sampling path, each block consists of two Conv2d layers, two Batch Norm layers, and a ReLU layer. To avoid gradient disappearing, skip additions are widely used. In the up-sampling path, each block consists of a Batch Norm layer, two Conv2d layers and 3 ReLU layers. In the GN, the loss function is defined as:

$$l_{GN} = L_1\{I_{CI}, G\} + \lambda \times TV\{G\} + \alpha \times (1 - D(G))^2, \quad (3)$$

where $L_1\{.\}$ is the absolute difference between the GN output image and its 'ground truth', TV{.} stands for the total variation regularization that is being applied to the generator output, and the last term reflects a penalty related to the discriminator network prediction of the generator output [26]. The GAN was implemented using TensorFlow framework version 2.1 and Python version 3.7. We implemented the software on a desktop computer with a Core i7-7700 K CPU @ 4.2 GHz (Intel) and 64 GB of RAM. The network training and testing were performed using GeForce GTX 1080Ti GPUs (NVIDA).

3. Experiments

3.1. Material and setup

The demo setup of our smart-phone phase contrast microscope is shown in Fig. 7. The 3D design in Fig. 7(a) is developed on the basis of the 2D theorem schematic in Fig. 2(a). The portable microscope in Fig. 7 (c) is with a 3D size of 12 cm × 10 cm × 17 cm, and the weight is only ~ 400 g. A blue LED (JXLED3WB, JUXIANG Optics, China) with the power of 3 W is used as the quasi-monochromatic illumination. The singlet lens is fabricated by the cooperation of Nanjing University of Science & Technology (NUST) and Soochow University. And the material of our aspheric singlet lens is E48R, which is provided by ZEON Corp, JAPAN. The bio-sample is on a 3D printed holder, which is fixed on a XYZ axial fine adjuster (XR25C/M, ZHISHUN, China). The resolution of XYZ axial adjuster is 10 μm. The position of the singlet aspherical lens can be adjusted by a Z-axis translation stage (XR25C/M, ZHISHUN, China). The structural shell of our microscope is fabricated by 3D print technology (printed by NUST, China).

The bio-sample is processed in the lab of Suzhou Municipal Hospital (SMH). The tumor tissues are sliced into ~2–4 μm section. Half of them are unstained, and the others are stained with H&E. All the bio-samples used in this study were obtained from the SMH. They were prepared from existing specimen, following de-identification of the basic clinical information. Therefore, this work did not interfere with standard practices of diagnosis and treatment. These samples are all approved and supervised by the Medical Ethics Committee of SHM. These tumor tissue sections are then baked at 68 °C for 30 min to prevent falling and deparaffinized through xylene, absolute and 95% alcohols to distilled water. After bio-samples preparation, the sections are dyed with hematoxylin and eosin in turn, dehydrated through graded ethanol solutions and cleared with xylene. Finally, the H&E stained and unstained slides are sealed with a half drop of neutral resin gum and covered with a coverslip.

3.2. Results

Following the data collection, image registration, deep learning deconvolution and deep learning style-transfer, we would get virtual phase contrast microscopy for transparent bio-sample, i.e., unstained/transparent tumor tissue pathological slide, and H&E stained tumor tissue pathological slide. Figs. 8 and 9 visually demonstrate the high-fidelity performance of the GAN-based virtual phase contrast microscopy. We use the structural similarity (SSIM) index as a standard to compare two sets of images.

Fig. 8 (a) is the Zernike phase contrast image for the unstained tumor tissue, collected by the research-level microscope (NIB 900, NOVEL, CHINA). Fig. 8 (b) is the image recorded by the smart-phone microscope. Fig. 8 (c) is the virtual phase contrast image by deep learning style-transfer method. Fig. 8 (d) is the image under the brightfield mode of the research-level microscope (NIB 900), where the unstained transparent bio-sample cannot be observed. The SSIM between the Fig. 8 (b) and Fig. 8(a) is 0.53, while the SSIM between the Fig. 8 (c) and Fig. 8(a)

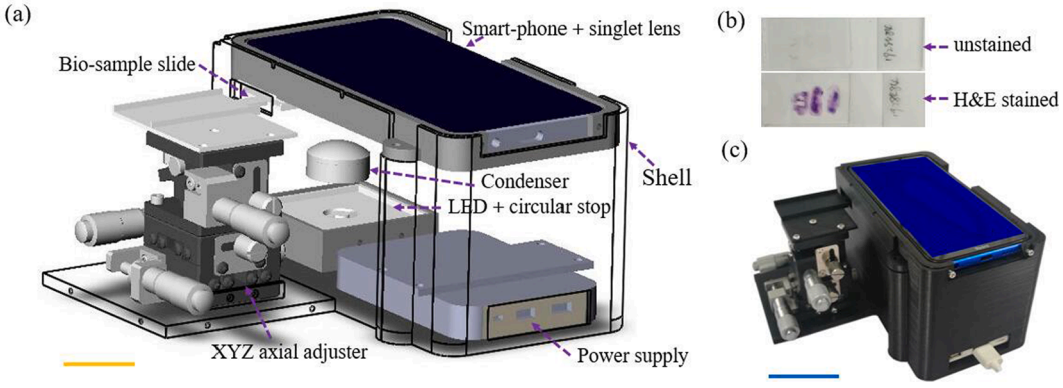

Fig. 7. Demo setup of our smart-phone phase contrast microscope. (a) 3D design diagram, the yellow scale bar is ~3 cm. (b) Photographs of unstained and H&E stained tumor tissue slides, which are with a size of 75 mm*25 mm*1mm. (c) Photograph of our smart-phone phase contrast microscope, the blue scale bar is ~5 cm.

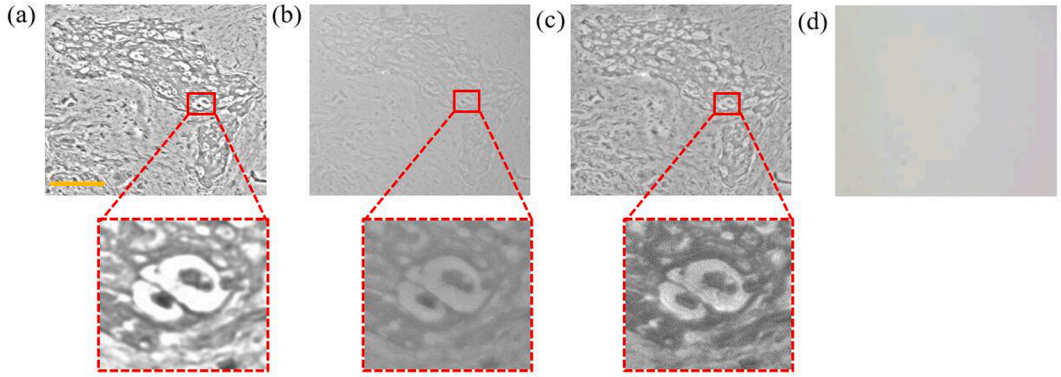

Fig. 8. Style-transfer virtual phase contrast image of unstained tumor tissue. (a) Zernike phase contrast image collected by a research-level microscope (NIB 900). (b) Greyed and deconvoluted image recorded by the smart-phone microscope. (c) Virtual phase contrast image by deep learning style-transfer method. (d) Brightfield image collected by a research-level microscope (NIB 900). The yellow scalar bar is ~50 μm.

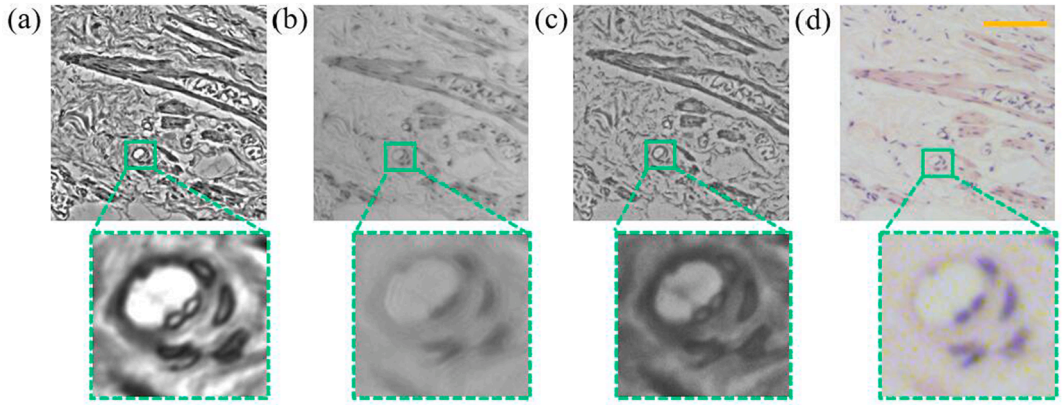

Fig. 9. Style-transfer virtual phase contrast image of H&E stained tumor tissue. (a) Zernike phase contrast image collected by a research-level microscope (NIB 900). (b) Greyed and deconvoluted image recorded by the smart-phone microscope. (c) Virtual phase contrast image by deep learning style-transfer method. (d) Colorful brightfield image collected by a research-level microscope (NIB 900). The yellow scalar bar is ~100 μm.

is improved up to 0.72.

Fig. 8 shows the phase contrast microscopy performance for totally transparent pathological tissue slide by our methods. In traditional staining pathological diagnosis, H&E staining and brightfield microscopy are viewed as a gold-standard and a routine by hospital. Here, we also use a H&E stained tissue slide to show our methods' imaging performance. Fig. 9(a) is the Zernike phase contrast image for the H&E stained tumor tissue, collected by the research-level microscope (NIB 900). Fig. 9(b) is the image recorded by the smart-phone microscope. Fig. 9(c) is the virtual phase contrast image by deep learning style-transfer method. Fig. 9(d) is the colorful bio-sample image under the brightfield mode of the research-level microscope (NIB 900). The SSIM between the Fig. 9(b) and Fig. 9(a) is 0.59, while the SSIM between the Fig. 9(c) and Fig. 9(a) is improved up to 0.71.

Actually, in the computational imaging part, it is a deep learning style-transfer method to transfer the phase contrast style onto an oblique illumination microscopy image. When a totally transparent bio-sample is in a brightfield illumination, such as Fig. 8(d), the background light is very strong and the signal light modulated by the transparent object is very weak. Background light and low-frequency is strong, but with less useful information. However, the circular oblique illumination helps suppressing the strong background light. Under circular oblique illumination, the edge and refractive index changes would be highlights. The extreme situation of circular oblique illumination is the dark-field microscopy, which has been widely used to observe high-frequency details, which ignoring the low-/middle- frequency information. By the way, our virtual phase contrast microscopy is a style-transfer deep convolution. It can enhance the image contrast in visual sense, but cannot create new information. Thus, it fails to transfer the brightfield images (i.e., Fig. 8(d)) of transparent bio-sample into the phase contrast style.

4. Discussion

Apparently, our singlet objective lens is free from assembling and precise packaging, which means a further low cost in the industrial producing compared with the commercial microscope objective lens. But its PSF is less sharp than the commercial microscope objective lens, which would be deconvoluted by the computational imaging method [26]. Besides, to achieve portability and compactness, our singlet objective lens is fixed before the rear camera of the smart-phone where there is only one microscopy magnification. And our portable smart-phone microscope could not be coupled with more functions, such as fluorescent imaging. These are our disadvantages, since the commercial microscopes are with multiple imaging magnifications and could be easily coupled with different functional modules.

In optics design, the singlet aspheric lens is designed for the cell-phone camera module, whose parameters are following. The focal length is 10 mm, the F# is 1.79 and the CMOS image sensor is with 0.8 μm pixel size and 1/2 in. area. Thus, if a smart-phone camera's F# is lager than 1.8, and the focal length is shorter than 10 mm. Our aspheric singlet lens is still fit. Otherwise, field vignetting and aperture mismatching would exist.

In the aspect of price and cost, the camera lens is ~USD1-10 / RMB 7-

100, which have been shown in Refs. [5,12–15]. This low price is based on the mass industrial production. The industrial chains about the aspheric lens manufacturing and assembling are very expensive and need large labors. A camera lens is compound of ~7 pieces of singlet aspheric lens, and they are all assembled precisely. In contrast, our singlet lens is free from precise assembling, which means only 14% cost and even less.

Comparing with other kinds of high freedom degrees surface, e.g., non-uniform rational B-spline surface, Q-type surface, Zernike surface, and meta surface, the even aspheric surface is the easiest to fabricate. But more freedom degrees mean a chance to get a better PSF. Actually, in reported meta-surface lens microscopy [40], good PSF microscopy imaging has been achieved. Although a sharper PSF means a better resolution ability, its property of the linear signal system is the key thing and a low-cost price is very meaningful. Therefore, the even aspheric lens made of the plastic material is our best choice.

The smart-phone is with a CPU and may also have a GPU, but our deep learning deconvolution and image-style-transfer are all executed on the bench-top computer. The bench-top computer is with a Core i7-7700K CPU @ 4.2 GHz (Intel), 64 GB of RAM, a Windows 10 operating system (Microsoft) and GeForce GTX 1080Ti GPUs (NVIDA). The reasons of using a bench-top computer are following. Firstly, in the assumed applications, the smart-phone phase contrast microscopes are to record image data, then tele-transmit them, by a WIFI/5G+ telecommunication network, to a medical data analysis center. The medical data analysis center, with a server computer, would provide data calculation, analysis, even and diagnosis advices. Secondly, the data processing ability and speed of a smart-phone are both always far less than a bench-top computer and a server computer. Thirdly, without the consideration of processing data, a cheaper smart-phone could be chosen.

5. Conclusion

In this manuscript, we propose a novel method to achieve phase contrast microscopy for medical diagnosis based on the smart-phone. Two highlights are presented. One is the customized aspheric singlet. It is with linear signal imaging properties across all FOVs by controlling its NMTFs. And the other is the computational imaging method, i.e., deep learning style-transfer methods. By the deep learning enhancing, the directly recorded circular oblique illumination images are converted into a phase contrast image virtually. There is no birefringent prism and inset phase plate in our setup. Proved by experiments with unstained transparent tumor tissue slides and H&E stained tumor tissue slides, the SSIMs and the visual contrasts are both improved much. Our results provide a powerful example of the low-cost portable phase contrast microscope with high-speed tele-communication abilities in the 5G+ mobile internet era. In assumed applications, our portable smart-phone phase contrast microscope is suitable for unstaining and transparent biological detection, wild field test and high-contrast observing transparent bio-medical tissues. Besides, it is also suitable for mobile health care, remote on-line biological teaching, remote on-line biological experimental course and so on [41].

Declaration of Competing Interest

All authors declare that they have no conflict of interest.

Acknowledgments

This study is partially supported by the Basic Research Program of Jiangsu Province (BK20190456, BK20201305), National Natural Science Foundation of China (NSFC) (62005120), the Fundamental Research Funds for the Central Universities (30919011261), Beijing Satellite Environmental Engineering Institute (CAST-BISEE2019-038), Chinese Academy of Sciences (KLOMT190101) and the National Key Research and Development Program (2019YFB2005500).

References

[1] K. Chu, Z.J. Smith, A.R. Espenson, D. Dwyre, S. Lane, D. Matthews, S. Wachsmann-Hogiu, Microscopy and Spectroscopy on a Cell Phone, Frontiers in Optics 2011/Laser Science XXVII, Optical Society of America, San Jose, California, 2011 p. JWA8.
[2] K. İçöz, Image processing and cell phone microscopy to analyze the immunomagnetic beads on micro-contact printed gratings, Appl. Sci. 6 (10) (2016).
[3] R.R. Jahan-Tigh, G.M. Chinn, R.P. Rapini, A comparative study between smartphone-based microscopy and conventional light microscopy in 1021 dermatopathology specimens, Arch. Pathol. Lab. Med. 140 (1) (2016) 86–90.
[4] I.I. Bogoch, J. Lundin, N.C. Lo, J.R. Andrews, Mobile phone and handheld microscopes for public health applications, Lancet Public Health 2 (8) (2017), e355.
[5] H.C. Koydemir, A. Ozcan, Mobile phones create new opportunities for microbiology research and clinical applications, Fut. Microbiol. 12 (8) (2017) 641–644.
[6] U.P. Moravapalle, A. Deshpande, A. Kapoor, R. Ramjee, P. Ravi, Blood Count on a Smartphone Microscope: Challenges, Proceedings of the 18th International Workshop on Mobile Computing Systems and Applications, Association for Computing Machinery, Sonoma, CA, USA, 2017, pp. 37–42.
[7] G. Muyo, A. Singh, M. Andersson, D. Huckridge, A. Wood, A.R. Harvey, Infrared imaging with a wavefront-coded singlet lens, Opt. Express 17 (23) (2009) 21118–21123.
[8] F. Languy, K. Fleury, C. Lenaerts, J. Loicq, D. Regaert, T. Thibert, S. Habraken, Flat Fresnel doublets made of PMMA and PC: combining low cost production and very high concentration ratio for CPV, Opt. Express 19 (S3) (2011) A280–A294.
[9] R.G. González-Acuña, H.A. Chaparro-Romo, General formula for bi-aspheric singlet lens design free of spherical aberration, Appl. Opt. 57 (31) (2018) 9341–9345.
[10] J. Nagar, S.D. Campbell, D.H. Werner, Apochromatic singlets enabled by metasurface-augmented GRIN lenses, Optica 5 (2) (2018) 99–102.
[11] Y. Peng, Q. Sun, X. Dun, G. Wetzstein, W. Heidrich, F. Heide, Learned large field-of-view imaging with thin-plate optics, ACM Trans. Graph. 38 (6) (2019). Article 219.
[12] J.-H. Kim, H.-G. Joo, T.-H. Kim, Y.-G. Ju, A smartphone-based fluorescence microscope utilizing an external phone camera lens module, Biochip J. 9 (4) (2015) 285–292.
[13] A. Orth, E.R. Wilson, J.G. Thompson, B.C. Gibson, A dual-mode mobile phone microscope using the onboard camera flash and ambient light, Sci. Rep. 8 (1) (2018) 3298.
[14] S. Pechprasarn, P. Pimonsakonwong, P. Kulikhandan, P. Suvarnaphaet, W. Pongruengkiat, P. Suksan, N. Albutt, Compact fluorescence microscope for smartphone and tablet, Appl. Mech. Mater. 879 (2018) 222–226.
[15] O. Yuma, S. Ryo, M. Ryoji, A. Hidenobu, T. Yosuke, W. Wataru, Mobile-phone-based Rheinberg microscope with a light-emitting diode array, J. Biomed. Opt. 24 (3) (2018) 1–6.
[16] C. Maurer, A. Jesacher, S. Bernet, M. Ritsch-Marte, Phase contrast microscopy with full numerical aperture illumination, Opt. Express 16 (24) (2008) 19821–19829.
[17] S.B. Mehta, C.J.R. Sheppard, Partially coherent image formation in differential interference contrast (DIC) microscope, Opt. Express 16 (24) (2008) 19462–19479.
[18] Y. Wu, Y. Zhang, W. Luo, A. Ozcan, Demosaiced pixel super-resolution for multiplexed holographic color imaging, Sci. Rep. 6 (1) (2016) 28601.
[19] J. Dou, Z. Gao, J. Ma, C. Yuan, Z. Yang, D. Claus, T. Zhang, Phase retrieval based on pupil scanning modulation, Appl. Phys. B 123 (8) (2017) 217.
[20] M. Niu, G. Luo, X. Shu, F. Qu, S. Zhou, Y.-P. Ho, N. Zhao, R. Zhou, Portable quantitative phase microscope for material metrology and biological imaging, Photon. Res. 8 (7) (2020) 1253–1259.
[21] Y. Fan, J. Sun, Q. Chen, X. Pan, L. Tian, C. Zuo, Optimal illumination scheme for isotropic quantitative differential phase contrast microscopy, Photon. Res. 7 (8) (2019) 890–904.
[22] J. Zhu, R. Zhou, L. Zhang, B. Ge, C. Luo, L.L. Goddard, Regularized pseudo-phase imaging for inspecting and sensing nanoscale features, Opt. Express 27 (5) (2019) 6719–6733.
[23] A. Pan, C. Zuo, B. Yao, High-resolution and large field-of-view Fourier ptychographic microscopy and its applications in biomedicine, Rep. Prog. Phys. 83 (9) (2020), 096101.
[24] A. Pan, Y. Zhang, K. Wen, M. Zhou, J. Min, M. Lei, B. Yao, Subwavelength resolution Fourier ptychography with hemispherical digital condensers, Opt. Express 26 (18) (2018) 23119–23131.
[25] A. Pan, Z. Chao, X. Yuege, L. Ming, Y. Baoli, Vignetting effect in Fourier ptychographic microscopy, Opt. Lasers Eng. 120 (2019) 40–48.
[26] H. Shen, J. Gao, Portable deep learning singlet microscope, J. Biophotonics 13 (6) (2020), e202000013.
[27] T. Nguyen, K. Mori, R. Thawonmas, Image Colorization Using a Deep Convolutional Neural Network, 2016.
[28] T. Abraham, A. Shaw, D. O'Connor, A. Todd, R. Levenson, Slide-free MUSE Microscopy to H&E Histology Modality Conversion via Unpaired Image-to-Image Translation GAN Models, 2020, p. arXiv:2008.08579.
[29] X. Dun, H. Ikoma, G. Wetzstein, Z. Wang, X. Cheng, Y. Peng, Learned rotationally symmetric diffractive achromat for full-spectrum computational imaging, Optica 7 (8) (2020) 913–922.

[30] W. He, J. Dou, Z. Yang, Z. Liu, Z. Liu, Sequential shift absolute phase aberration calibration in digital holographic phase imaging based on chebyshev polynomials fitting, IEEE Photonics J. 12 (1) (2020) 1–11.
[31] H. Liang, K.N. Plataniotis, X. Li, Stain style transfer of histopathology images via structure-preserved generative learning, 2020, p. arXiv:2007.12578.
[32] D. Mahapatra, B. Bozorgtabar, J.-P. Thiran, L. Shao, Structure preserving stain normalization of histopathology images using self-supervised, Semantic Guidance (2020) p. arXiv:2008.02101.
[33] Y. Rivenson, T. Liu, Z. Wei, Y. Zhang, K. de Haan, A. Ozcan, PhaseStain: the digital staining of label-free quantitative phase microscopy images using deep learning, Light Sci. Appl. 8 (1) (2019) 23.
[34] Y. Rivenson, H. Wang, Z. Wei, K. de Haan, Y. Zhang, Y. Wu, H. Günaydın, J. E. Zuckerman, T. Chong, A.E. Sisk, L.M. Westbrook, W.D. Wallace, A. Ozcan, Virtual histological staining of unlabelled tissue-autofluorescence images via deep learning, Nat. Biomed. Eng. 3 (6) (2019) 466–477.
[35] N. Singla, V. Srivastava, Deep learning enabled multi-wavelength spatial coherence microscope for the classification of malaria-infected stages with limited labelled data size, Opt. Laser Technol. 130 (2020), 106335.
[36] H. Byeon, T. Go, S.J. Lee, Deep learning-based digital in-line holographic microscopy for high resolution with extended field of view, Opt. Laser Technol. 113 (2019) 77–86.
[37] M.T. Shaban, C. Baur, N. Navab, S. Albarqouni, Staingan: Stain Style Transfer for Digital Histological Images, 2019 IEEE 16th International Symposium on Biomedical Imaging (ISBI 2019), 2019, pp. 953-956.
[38] Y. Rivenson, K. de Haan, W.D. Wallace, A. Ozcan, Emerging advances to transform histopathology using virtual staining, BME Frontiers 2020 (2020) 9647163.
[39] Y. Zhang, K. de Haan, Y. Rivenson, J. Li, A. Delis, A. Ozcan, Digital synthesis of histological stains using micro-structured and multiplexed virtual staining of label-free tissue, Light Sci. Appl. 9 (1) (2020) 78.
[40] C. Chen, W. Song, J.-W. Chen, J.-H. Wang, Y.H. Chen, B. Xu, M.-K. Chen, H. Li, B. Fang, J. Chen, H.Y. Kuo, S. Wang, D.P. Tsai, S. Zhu, T. Li, Spectral tomographic imaging with aplanatic metalens, Light Sci. Appl. 8 (2019) 99.
[41] L.C. Wicks, G.S. Cairns, J. Melnyk, S. Bryce, R.R. Duncan, P.A. Dalgarno, EnLightenment: high resolution smartphone microscopy as an educational and public engagement platform, Wellcome Open Res. 2 (2017) 107.